USING A SINGLE SHOT SPECTROMETER TO DETERMINE THE SPECTRAL CHARACTERISTICS OF THE BEAM AS A RESULT OF MICRO-BUNCHING INSTABILITIES*

A. Finn†, JAI at Royal Holloway University of London, UK & Diamond Light Source, UK
P. Karataev, JAI at Royal Holloway University of London, UK
G. Rehm, Diamond Light Source, UK

Abstract

A single-shot spectrometer has been designed and is in operation at the Diamond Light Source (DLS). It is an array of eight Schottky barrier diodes (SBDs) each with a distinct frequency band covering 33-1000 GHz. The aim of the spectrometer is to observe the bursts of coherent synchrotron radiation (CSR) as a result of micro-bunching instabilities (MBI) and stable low alpha modes, where alpha is the momentum compaction factor. In this case, the bursts of CSR occur with wavelengths in the mm regime. SBDs are often implemented as detectors in the millimetre wavelength range and benefit from low noise, excellent sensitivity and ultra-fast responses. The eight SBDs have been individually characterised thus making the results obtained comparable to simulations. Here we present, an analysis of the data obtained via the spectrometer in particular, the bursting nature and spectral characteristics of a sample of beam modes at DLS. Furthermore, the results obtained can be used to confirm simulations.

INTRODUCTION

Micro-bunch instabilities (MBI) occur when the charge of a single bunch exceeds a threshold current and the bunch begins to filament [1]. This can occur by reducing the size of the bunch or by adding more electrons to the bunch. The filaments, or 'micro-bunches', created go on to emit coherent synchrotron radiation (CSR) in the THz (mm) range. Incoherent synchrotron radiation has linear relationship with an increase in current, however CSR goes as the square. The CSR from the micro-bunches occurs as intense bursts on ever-changing timescales, and with unstable intensities. It must be noted that CSR only occurs at wavelengths longer than the bunch. However, when CSR is produced as a result of MBI the wavelength can be shorter than the bunch length but must be the same size or longer that the bunch filament emitting it. This means that the wavelength can be much shorter than the entire bunch length.

These MBI have been observed at many synchrotron light sources internationally including Diamond Light Source [2], BESSY-II [3, 4], SURF-II [5], NSLS VUV [6, 7], ALS [8], UVSOR-II [9] and MAX-I [10]. Many synchrotrons are utilising a variety of different methods to investigate the CSR produced as a result of the MBI and what this implies. Here at the Diamond, a single-shot spectrometer is installed at a dedicated viewport containing eight channels, covering a frequency range of 33-1000 GHz with the capability to obtain turn-by-turn data from the synchrotron storage ring. By measuring the CSR spectrum in a single shot we can deduce information about the micro-bunch structure and its turn-by-turn evolution.

Data has been captured in a variety of beam modes: normal mode and two varieties of 'low-alpha' mode whereby the momentum compaction factor, α, is reduced. Normal mode (NM) uses $\alpha_{user} = 1.7e{-}04$ but the low-alpha modes (LAM) set $\alpha_{THz} = -4.5e-06$ and $\alpha_{Pulse} = -1e-05$. By reducing α, the bunches become compressed, this creates shorter bunches and thus shorter light pulses which can be used for time resolved or pulse-probe experiments. This setting allows for stable CSR. When $\alpha_{THz} = -4.5e-06$, the bunch is further compressed but this allows for the charge of a bunch to exceed the threshold and CSR bursting to occur. At Diamond the CSR bursts appear at mm-wavelengths and thus beamlines dedicated to THz research benefit from this synchrotron radiation.

SBD SPECTROMETER

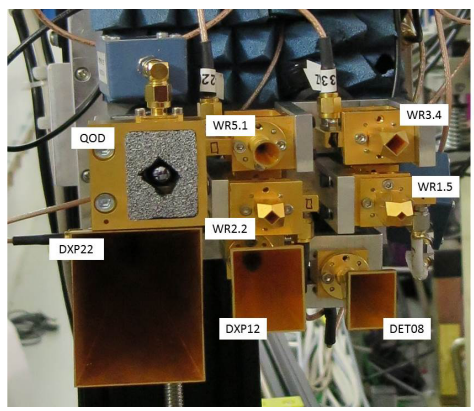

Figure 1: Layout of detector array plate.

The single-shot spectrometer is a detector array, containing eight zero-biased SBDs spanning 33-1000 GHz, as shown in Figure 1. Of the eight SBDs, seven are housed within waveguides and are thus frequency restricted. Horn antennas guide the radiation to the the diodes within these detectors. The eighth is a broadband quasi-optical detector (QOD) with a silicon lens. SBDs were chosen due their low noise, excellent sensitivity and fast response [11]. These

* The research leading to these results was funded by Diamond Light Source, and Royal Holloway, University of London
† aiveen.finn.2013@live.rhul.ac.uk

ISBN 978-3-95450-147-2

detectors operate at room temperature, thus they are more compact and economical. All eight detectors are positioned to be as close together as possible to observe the most signal simultaneously with all entrance apertures in the same plane to eliminate any shadowing. Characterisations of all eight detectors and corresponding horn antennas (if applicable) in the forward direction have been carried out on the test bench [12] and thus the power of the radiation detected can be determined.

Table 1: SBD Sensitivity Characteristaions

Detector Model	Stated Range GHz	Sensitivity per Area V/(W/m^2)
DXP-22 [13]	33-50	1.77
DXP-12 [13]	60-90	0.55
DET-08 [13]	90-140	0.25
WR5.1ZBD [14]	140-220	0.07
WR3.4ZBD [14]	220-330	0.02
WR2.2ZBD [14]	330-500	0.02*
WR1.5ZBD [14]	500-750	0.004*
QOD [14]	100-1000	0.04

where * means reverse-calculated

The SBD array is placed on a three-way motion stage set-up in front of the silica window of the beamport dedicated to the investigations of CSR from MBI [15]. The viewport is designed to guide the synchrotron radiation from bending magnet B06 to the viewport window while removing x-ray radiation by way of water-cooled copper mirrors. In order to boost the signals from the detectors before traversing 30 m of cable to the data acquisition unit, each SBD is terminated into its own voltage amplifier with a high impedance (10 kΩ) to take full advantage of the excellent sensitivity these detectors have to offer [12]. The signals are fed into a simultaneous multi-channel digitiser which constantly streams out data into a local server. The server carries out FFTs of the data selecting a region of interest around the revolution frequency of the storage ring (533.820 kHz) and then performs a power average over every ten data sets for each of the eight channels [12].

The analysis presented here concentrates primarily on the highest frequency bandwidth limited detector in the array. The WR1.5ZBD (500-750 GHz) from Virginia Diodes Inc. [14] covers the largest bandwidth of the frequency restricted SBDs. Its true waveguide limits are 393.70-787.40 GHz given by the fundamental (i.e. TE_{10}) mode cut off of the waveguide and the lower cut off of the frequency of the next mode. This detector was procured because interesting activity had been seen with the next highest frequency detector WR2.2ZBD (330-500 GHz).

RESULTS

Due to the nature of the data acquisition system implemented here, the Fourier transformed data is continually streamed from the server. This allows for changes to the mm spectrum to be monitored in real time. As the region of interest is the centered around the revolution frequency of Diamond, the most prominent signal is at 533.820 kHz, as can be seen in Figure 2.

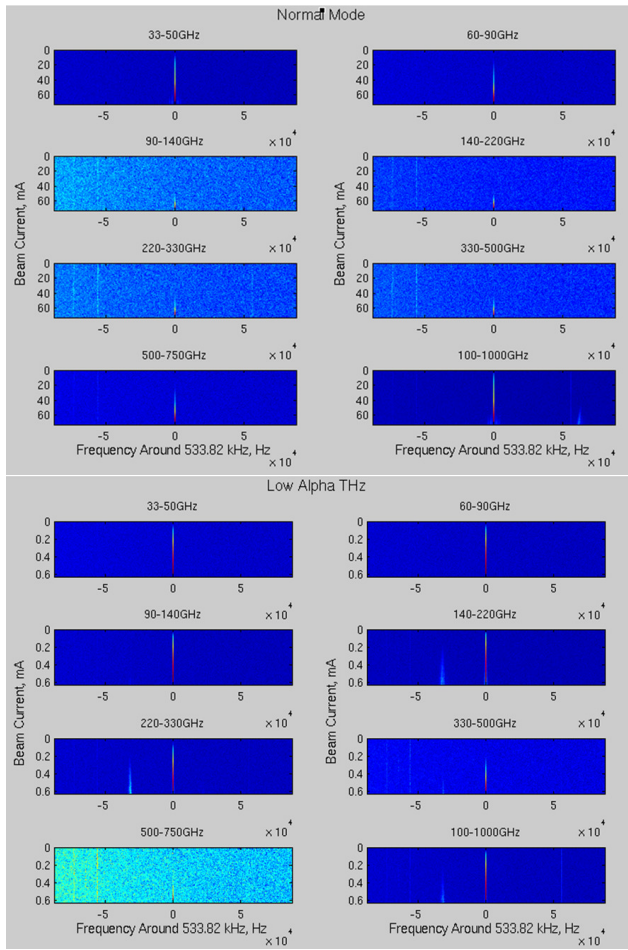

Figure 2: The change of signal strength with an increase of current for Normal Mode (above) and Low Alpha Mode (below) with multi-bunch fills.

It is interesting to note that the 500-750 GHz detector is one of the four which detects the most amount of signal in NM, however in LAM it detects the least. This is not to be expected. The beam is expected to have a gaussian distribution in both NM and LAM. Thus the detectors should be observing less and less the higher in frequency they are able to detect. In the case of the NM, this is especially true. The signal observed by the 500-750 GHz detector is known to be coming from the tail of the bunch form-factor. However, because the signal is strongly detected it implies that the distribution is not entirely gaussian.

The beamport though dedicated to MBI research has not been optimised for the extraction of mm-wavelength and thus a limiting vertical aperture of 11.5 mm exists soon after the source of the bending magnet radiation. Concentrating on the case of NM, it could be thought that the limiting aperture is sufficient to allow all of the 500-750 GHz worth of radiation through without clipping, while the lower frequencies are more affected by the aperture. It can be clearly seen on

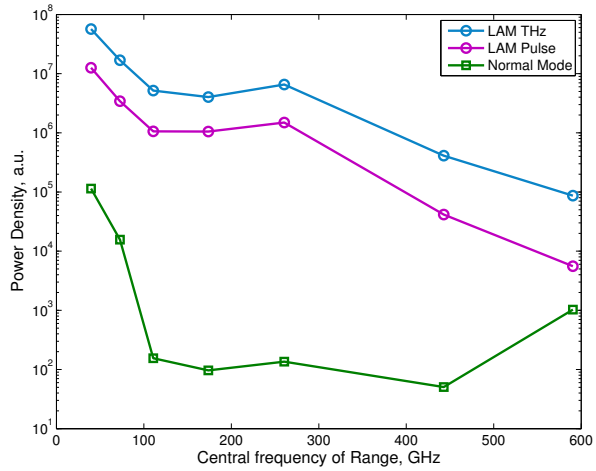

Figure 3: Spectral power density for the Normal Mode (green squares) and Low Alpha Modes (blue and magenta circles) with respect to the central frequency for each of the seven detectors.

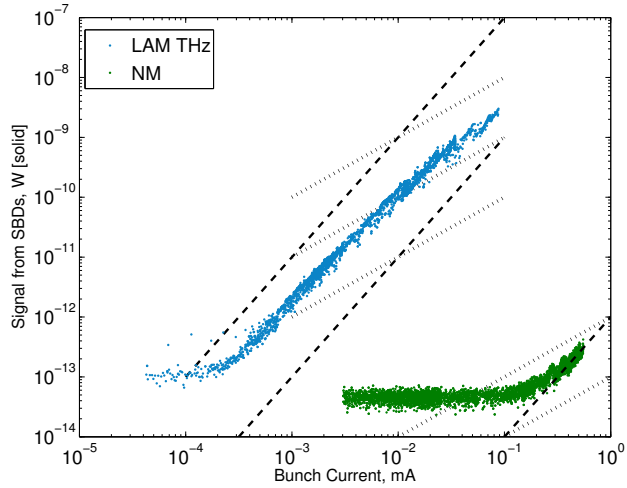

Figure 4: Relationship between signal observed by the 500-750 GHz detector and the bunch current for Normal Mode (green) and Low-Alpha Mode for THz (blue), where quadratic lines are dashed and linear dotted.

the spectral power density plot (Figure 3) that the NM curve distinctly rises for the 500-750 GHz detector, despite the overall decline. This is in agreement with the bunch distribution not being gaussian. The assumption that the aperture is affecting the results is not supported by the LAM data as the power density value for the seventh detector follows the decline.

In Figure 3, it is expected that the LAM cases experience a higher power density. This is because LAM is designed to either produce compressed bunches for shorter light pulses which leads to stable CSR or else to specifically create bursting CSR in order to obtain a high flux of mm radiation. As the detectors are designed for mm-wavelengths, naturally they observe more activity at these wavelengths. It can be seen that LAM for THz conditions provides the highest spectral power density, as anticipated. The spectral power density was ascertained by using the signal obtained for each detector for the entire raster scan at a fixed longitudinal position. The discrepancy in the ratio between NM and LAM THz from Figures 3 and 4 is because the spectral power density takes into account the entire x-y area while the current ramp only observes data at the optimal position. Furthermore, it is from the raster scans that the optimal position of detector array is established for each necessary longitudinal position.

The signal from the 500-750 GHz detector obtained at the revolution frequency (533.820 kHz) for the optimal positioning of the detector array is displayed in Figure 4. The data were treated with the previously determined sensitivity factors with effective apertures and thus the true signal was determined in watts [12]. For the NM case, the 500-750 GHz detector takes a long time to rise, especially in comparison to the LAM THz mode. This again infers that NM has less of a THz signal than LAM. Both NM and LAM cases have a quadratic dependence and are thus in keeping with what is expected of the MBI CSR bursts. At the highest currents, the LAM THz curve begins to lose its quadratic dependence becoming more linear. This is as a result of the SBD beginning to saturate and is being driven into its linear regime.

CONCLUSIONS

The eight channel SBD array is installed and fully operational at Diamond. It has been collecting data for a variety of beam modes. The 500-750 GHz detector brings to attention the differences between the NM and LAMs in particular the assumed gaussian bunch distribution. Deeper analysis is required to fully understand what is occurring, especially with regards the NM.

ACKNOWLEDGEMENT

A Finn would like to thank IPS Martin for providing Low Alpha Conditions and for the use of his scripts. The IoP have contributed to the cost of attending IPAC'16.

REFERENCES

[1] Venturini, M., Warnock, R. L., et al., 2005, PRST-AB, Vol. 8, Issue 1, p 014202.

[2] Rehm, G., et al., 2009, DIPAC Proceedings, TUPD32.

[3] Abo-Bakr, M., Feikes, J., et al., 2002, Phys Rev Lett, Vol. 88, Issue 25, p 254801.

[4] Kuske, P., 2009, PAC, FR5RFP063.

[5] Hight Walker, A. R., Arp, U., et al., 1997, SPIE Proceedings,Vol. 3135, pp 42-50.

[6] Podobedov, B., Carr, G. L., et al., 2001, PACS Proceedings, pp 1921-1923.

[7] Carr, G. L., Kramer, S. L., et al., 2001, NIM A, Vol. 463, pp 387-392.

[8] Byrd, J. M., Leemans, W. P., et al., 2002, Phys Rev Lett, Vol. 89, Issue 22, p 224801.

ISBN 978-3-95450-147-2

[9] Mochihashi, A., Hosaka, M., et al., 2006, EPAC Proceedings, THPLS042.

[10] Andresson, A., Johnson, M. S., et al., 2000, Opt Eng, Vol. 39, Issue 12, pp 3099-3105.

[11] Smith, R. J., Dorf, R. C., 1992, *Circuits Devices and Systems*, Wiley & Sons Inc.

[12] Finn, A., et al., 2016, J. Phys. Conf Ser.,'in press', RREPS2015.

[13] Millitech Inc, Detector Specifications, Millimeter-Wave Technology & Solutions.

[14] Virginia Diodes Inc., VDI User Guide.

[15] Shields, W., et al., 2012, IPAC Proceedings, WEPPR079.